International Journal of Pharmaceutics 414 (2011) 321–331

Contents lists available at ScienceDirect

International Journal of Pharmaceutics

journal homepage: www.elsevier.com/locate/ijpharm

Pharmaceutical Nanotechnology

Drug release characteristics from nanoclay hybrids and their dispersions in organic polymers

Jin Uk Ha[1], Marino Xanthos*

Otto H. York Department of Chemical, Biological and Pharmaceutical Engineering, New Jersey Institute of Technology, Newark, NJ 07102, USA

ARTICLE INFO

Article history:
Received 27 January 2011
Received in revised form 1 May 2011
Accepted 6 May 2011
Available online 12 May 2011

Keywords:
Controlled release
Melt mixing
Nanoclays
Aqueous solubility
Diffusion
Ion exchange

ABSTRACT

This study establishes and compares structure–property–processing relationships on three drug delivery systems containing an anionic active pharmaceutical ingredient (API) in the following excipient carriers: (a) an inorganic anionic nanoclay, (b) pH responsive acrylic polymers, and (c) combinations thereof. The effects of the excipients on the APIs dissolution rate were studied from their release profile in simulated body fluids (SBFs) with different pH.

In the API-nanoclay system, calcination of the clay followed by its reconstitution in an API solution was successfully used to intercalate the API in its amorphous state in the clay. As a result, the API showed increased apparent solubility vs. its crystalline form with its release mechanism from the clay being predominantly diffusion controlled and depending on the pH of the SBFs. In melt mixed ternary polymer systems containing the above hybrids, as a result of an additional diffusional step due to presence of nanoplatelets, the API showed a more controlled release vs. polymer systems that contained only API. By comparison to the low pH SBF, the ternary system in the pH 7.4 SBF showed a reduced diffusion contribution due to the presence of clay platelets, the latter unaffected by the high pH value. Reasonable agreement was found with predictions from literature diffusion/erosion models.

It is confirmed that hot melt mixing offers opportunities to produce systems with enhanced API apparent solubility. The presence of nanoclays can also increase the API's apparent solubility and affect its release in a controlled manner.

1. Introduction

Nanoclays in the form of high aspect ratio platelets are well known as high performance functional fillers for polymers, improving their mechanical, thermal, and barrier properties (Kamena, 2010; Schmidt et al., 2002). Clays can also be directly used for pharmaceutical applications. For example, a cationic montmorillonite nanoclay, MMT, is a potent detoxifier and it can adsorb dietary toxins, bacterial toxins associated with gastrointestinal disturbance and metabolic toxins such as steroidal metabolites associated with pregnancy (Dong and Feng, 2005; Guarino et al., 2001). Hydrotalcite, an anionic nanoclay – from the family of layered double hydroxides (LDHs) – is a popular antacid and is used because magnesium and aluminum metal oxides slowly hydrolyze regulating the pH to an optimum value without provoking a rebound effect in the stomach (Linares and Brikgi, 2006).

In addition to the therapeutic attributes of some unmodified nanoclays, their hybrids with ionic active pharmaceutical ingredients (APIs) that may be intercalated in the nanoclay interlayer space (Li et al., 2004a) in a non-crystalline, amorphous state can provide advantages such as: (a) increased apparent solubility of APIs with poor aqueous solubility, (b) controlled API release and, (c) improved bioavailabilty. It has been hypothesized (Aguzzi et al., 2007; Li et al., 2004a; Suzuki et al., 2001; White and Hem, 1983; Dong and Feng, 2005) that the addition of the nanoclay platelets may improve the overall API stability by providing a tortuous path that would slow down the API's diffusion to the body fluids in the presence or absence of a polymeric excipient. The decrease of the API's mobility inside the polymeric excipient would also help to prevent or slow down the aggregation of the API molecules. Thus, the crystallization of the API molecules that may lead to their delayed dissolution could be minimized and the long term drug stability improved. It should be noted that hydrophilic polymers are, in general, chosen

Abbreviations: AEC, anionic exchange capacity; API, active pharmaceutical ingredient; CHT, calcined hydrotalcite; DSC, differential scanning calorimetry; DIK, diclofenac; EDX, energy dispersive X-ray; FBF, benbufen; FTIR, Fourier transform infrared; HT, hydrotalcite; IND, indomethacin; LDH, layered double hydroxide; MMT, montmorillonite; SBF, simulated body fluid; SEM, scanning electron microscopy; SGF, simulated gastric fluid; TEC, triethyl citrate; TGA, thermogravimetric analysis; XRD, X-ray diffraction.

* Corresponding author. Tel.: +1 201 6424762; fax: +1 973 5968436.
E-mail addresses: jinuk.ha@samsung.com (J.U. Ha), xanthos@njit.edu (M. Xanthos).
[1] Present address: Chemical Research Institute, Samsung Cheil Industries Inc, Uiwang-Si 437-711, Republic of Korea.

0378-5173/$ – see front matter © 2011 Elsevier B.V. All rights reserved.
doi:10.1016/j.ijpharm.2011.05.028

as excipients for the purpose of improving the APIs' dissolution rate. It follows, then, that hydrophilic pharmaceutical nanoclays such as montmorillonite and hydrotalcite, would tend to disperse better in hydrophilic polymers due to their improved affinity.

Although some studies reported a decreased bioavailability of several APIs by co-administration with several types of clays (Vatier et al., 1994), concomitant benefits of the uses of nanoclays in modified drug delivery systems have been more often reported (Ambrogi et al., 2002; Costantino et al., 2008; Park et al., 2008; McGinity and Lach, 1977; McGinity and Harris, 1980). Modified drug delivery systems address issues such as release patterns and drug stability/targeting (Aguzzi et al., 2007).

The action mechanism of the API/Clay hybrids is believed to involve the following steps:

(1) The counter ion in the interlayer space of cationic or anionic clays can be exchanged with foreign ions (in this case charged API).
(2) The intercalated API/Clay complex is then able to ion exchange again at the action site and release API molecules.
(3) The released API from the clay interlayer space is absorbed at the action site and, thus, the API is functioning.

The following are some literature examples on specific combinations of anionic APIs and LDHs.

Li et al. (2004a) studied a fenbufen (FBF) delivery system produced by preparing FBF–LDH complexes through a co-precipitation method at different pH conditions. Fenbufen was successfully intercalated into the LDH interlayer as confirmed by XRD analysis. FBF content in LDH increased with increasing pH during co-precipitation. Release patterns were different in accordance with the presence of specific metal elements. An LDH composed of Mg/Al showed sustained API release, while the one containing Li/Al showed a maximum release within 20 min.

A study on dissolution of fenamates released from LDH was reported by Del Arco et al. (2008). Mefenamic and meclofenamic acid were intercalated into a chloride LDH interlayer by ion exchange. The intercalation of APIs was confirmed by X-ray diffraction (XRD) analysis. Dissolution of APIs from the LDH hybrids containing mefenamic was tested at three different pH of 1.2, 4.5 and 6.8. LDH-hybrids showed increased solubility at all three conditions. The authors attributed the increased solubility of the API from the LDH-mefenamic hybrid at pH 1.2 to the API released in its molecular form and to the dissolution of LDH under acidic conditions. Release profiles of all hybrids showed sustained API release as compared to pure APIs and API–LDH physical mixtures releases in the SBFs (pH 7.5 and 9). These slower releases were ascribed to ion exchange reactions between the API anion in the LDH interlayer and anions in the buffer solutions.

Co-precipitation and calcination methods were used for the intercalation of indomethacin (IND) into LDH by Del Arco et al. (2004). The expansion of the interlayer space of the modified LDH was confirmed by XRD. The co-precipitation method showed more IND loading (≈56 wt%) than the calcination method (≈25 wt%) in the LDH interlayer space and this was confirmed by elemental analysis. Pharmacological studies *in vivo* showed that mice that consumed the LDH modified with IND had reduced ulcerating damage as compared to the ones that were treated with IND alone.

For drug delivery applications, ternary systems consisting of polymers containing API intercalated nanoclays have been reported to provide interesting advantages as compared to binary polymer-API systems (Li et al., 2004b; Campbell et al., 2008; Bugatti et al., 2010; Ambrogi et al., 2002) such as a more controllable API release pattern as compared to binary systems; the ternary system has one more controllable parameter, namely the API release from the clay.

Among the objectives of this research are to determine the release characteristics of an ionic API, namely diclofenac sodium having pH dependent water solubility, from API–LDH hybrids into body fluid simulants and compare with its release when the same hybrids are dispersed in water soluble acrylate polymers by melt mixing. Melt mixing, in particular as applied to extrusion (known as HME, hot melt extrusion), has been reported to provide many advantages vs. conventional methods, such as increasing the API dissolution rate and thereby increasing the apparent solubility of drugs with poor solubility, elimination of solvent usage, and providing a continuous process (Liu et al., 2009; Crowley et al., 2004). Since, practically no data have been published on ternary systems produced by melt processing, this research opens the route for systems with improved efficacy, less toxicity and better patient compliance than conventional drug delivery devices.

2. Materials and methods

2.1. Materials

The API used in this study is the sodium salt of diclofenac $Cl_2C_6H_3NHC_6H_4CH_2COO^-Na^+$ (DIK-Na^+) purchased from Spectrum Chemical & Laboratory Products (Gardena, CA, USA). It is a white powder with molecular weight of 296.14 g/mol and melting point (T_m) of 284 °C. It is very soluble in methanol, whereas its aqueous solubility is low increasing with increasing pH (Kincl et al., 2004). The anionic LDH clay used in this work, referred to below as hydrotalcite, HT, is a synthetic aluminum magnesium hydroxyl carbonate donated by Sasol Germany (CAS # 11097-59-9, trade name: Pural MG 63 HT). It has a double layered metal hydroxide structure consisting of magnesium and aluminum hydroxide octahedrally interconnected via the edge; the manufacturer's reported weight ratio of Al_2O_3:MgO is 38:62. The chemical formula is $Mg_4Al_2(OH)_{12}CO_3{\cdot}nH_2O$, the basal spacing is 0.77 nm and the anionic exchange capacity (AEC) has been reported to be approximately 340 meq/100 g.

An amorphous cationic butyl/methyl methacrylate–dimethylaminoethyl methacrylate terpolymer (1:1:2) (Eudragit® E 100 granules) and an amorphous anionic methacrylic acid–methyl methacrylate (1:2) copolymer (Eudragit® S 100 powder) donated by Evonik Industries (Piscataway, NJ, USA), were used as the excipients of the APIs and the API modified clays. Eudragit® E 100 is soluble in the gastric fluid up to the pH 5.0. This polymer has a reported T_g of 48 °C, a maximum processing temperature of 220 °C and a reported density of 1.09 g/cm^3 (Six et al., 2002). Eudragit® S100 is soluble in the colonic fluid at pH above 7.0. This polymer has a reported T_g of 172 °C (Schilling et al., 2010) and a maximum processing temperature of 186 °C (Nollenberger et al., 2009). In order to facilitate the melt processing of Eudragit® S100 triethyl citrate (TEC) (Sigma–Aldrich) was used as a plasticizer. TEC is a colorless, odorless liquid with molecular weight 276.2 g/mol and density 1.137 g/cm^3. Its reported melting point is −55 °C and its boiling points are 127 °C at 1 mm Hg and 294 °C at 760 mm Hg. Reported solubility in water is 62 g/L (Budavari et al., 1996).

2.2. Modification of anionic nanoclays with DIK-Na^+

HT was calcined in a porcelain crucible heated at 490 °C for 7–8 h to remove volatiles, including carbon dioxide and water and produce calcined HT (CHT). CHT regeneration to a HT structure containing API anions instead of carbonate anions was carried out with methanol (200 ml) and de-ionized water (50 ml) solutions containing 2× the stoichiometric amounts of DIK based on the AEC of the HT. The solution pH was set to 6.0 by adding 0.05 N HCl. The reaction was carried out at 60 °C for 2 days in a closed system. The

modified clays, referred to as hybrids, were then filtered under vacuum, washed with a methanol/water mixture and separated from the solution by centrifuging. These washing procedures were repeated several times in order to remove the residual DIK from the clay surface. The modified clays were then dried at room temperature for 24 h and dried again at 80 °C for 24 h under vacuum.

2.3. Preparation of API/polymers and API/Clay/polymer compounds by melt mixing

Eudragit® E100 compounds containing 4 wt% or 15 wt% DIK-Na^+, or 10 wt% DIK/Clay hybrid (containing 4 wt% DIK) were prepared by compounding in a Brabender batch mixer (PL2000, C.W. Brabender, NJ, USA) at 50 rpm and 130 °C for 5 min. After melt mixing, the compounds were pressed for 50 s at 130 °C into thin disks for further analyses.

Eudragit® S100 was premixed with 20 wt% TEC in a wrist action shaker (Burrell Wrist-Action® Shaker) for 3 h. 4 wt% or 15 wt% DIK-Na^+, or 10 wt% DIK/Clay hybrid (containing 4 wt% DIK) were melt compounded with the premix in the batch mixer at 170 °C for 4 min. After compounding, samples were pressed into thin disks for further characterization.

2.4. Characterization

FTIR spectra of unmodified clays, APIs, API modified clays, polymer excipients with or without APIs, or API modified clays were obtained using a Spectrum One FTIR Spectrometer® (PerkinElmer Instruments, Waltham, MA, USA) in the mid-infrared range wavelength 400–4000 cm^{-1}. Thermogravimetric analysis (TGA) was carried out with a TGA Q50 analyzer (TA Instruments, New Castle, DE, USA). Tests were carried out from room temperature to 500 °C, at a heating rate of 20 °C/min in a nitrogen atmosphere (flow rate 40 cm^3/min). Glass transition temperature (T_g), melting temperatures (T_m) and other thermal properties were determined by differential scanning calorimetry (DSC) (DSC Q100, TA instruments). Heating and cooling rates were 20 °C/min in a nitrogen atmosphere. The weight of all test samples ranged from 4 to 9 mg. All samples were hot pressed and prepared as thin films before the analysis. T_g of samples was calculated from three DSC runs for each sample.

Wide-angle X-ray diffraction (XRD) analysis was performed with a Philips PW3040 diffractometer (Cu K_a radiation $\lambda = 0.154$ nm), operated at 45 kV/40 mA. All specimens were scanned in the 2θ range from 2° to 40° at a rate of 0.003°/s.

APIs, API modified clays and the fracture surfaces of polymer compounds were examined by scanning electron microscopy (LEO 1530 VP Emission SEM) at 3–5 keV working voltage. In order to identify the API and the clay particles and their degree of dispersion in the polymer matrix, energy dispersive X-ray analysis (EDX) (2400 PerkinElmer Elemental mapping), was used. By selecting characteristic elements, their mappings were possible and the detected elements were identified as dots. The working voltage was 5 kV and mapping time was 300 s for all specimens.

Elemental analysis of the hybrids for carbon, hydrogen, and nitrogen was performed at a contract Analytical Research and Development Laboratory (QTI Laboratories, Whitehouse, NJ, USA). The nitrogen content in the API modified HT was determined using a PerkinElmer 2400 Elemental Analyzer.

Drug dissolution (also referred to in the literature as drug release) was studied in a Distek (Distec Inc., North Brunswick, NJ) dissolution system 2100A at 36.5 ± 0.1 °C according to USP dissolution apparatus II with a paddle rotation speed of 50 rpm. The dissolution medium was 1 L of a pH 1.2 HCl buffer solution for simulating a gastric acid fluid and a pH 7.4 phosphate buffer solution for simulating a colonic fluid. The clay related dissolution tests were carried out with 100 ± 10 mg powders. Samples of the test fluid were collected at predetermined time intervals, filtered through a 0.45 μm filter and then analyzed at 276 nm for DIK-Na^+ by an UV–vis spectrophotometer (Evolution 60, Thermo Scientific). The experiments were repeated three times with good reproducibility. For dissolution tests of Eudragit® E100 and S100 compounds with APIs or API modified clays, 2 mm disks having the same circular holder geometry were produced by compression molding. The weight of each sample was 200 ± 20 mg.

3. Results and discussion

3.1. Characterization of clays modified with DIK-Na^+

3.1.1. FTIR results

FTIR spectra of DIK-Na^+, unmodified HT, and DIK/Clay are shown in Fig. 1. The spectra ascertain the presence of DIK on the clay but not its exact location. The anionic clay contains carbonate ions in its interlayer spacing corresponding to a band at 1357 cm^{-1} (Fig. 1(b)). The spectrum of the clay after calcination (CHT) and modification with DIK-Na^+ (Fig. 1 (c)) does not show a band at 1357 cm^{-1} indicating the successful removal of the carbonate ion from the interlayer space. On the DIK/Clay particles, the newly created peaks can be attributed to DIK that may be present as either a surface coating and/or as an intercalant. The peaks at 1575, 1508, 1499, and 1456 cm^{-1} indicate ring stretching of 1, 2, 3 tri-substituted benzene. The peak at 1585 cm^{-1} results from the benzene ring carbon–carbon vibration. The peaks at 1470 cm^{-1} and 1400 cm^{-1} correspond to the CH_2 bending of ortho-substituted benzene. The band in the region between 1300 and 1150 cm^{-1} is responsible for C–O bonds. The band for aryl halide between 1080 and 1060 cm^{-1} is not visible, apparently due to the strong interaction of ring vibrations (Colthup et al., 1975). The broad peak between 3700 and 3000 cm^{-1} results from hydroxyl groups of the layers and the reabsorbed interlayer water.

3.1.2. XRD results

XRD analysis was used to evaluate the intercalation of DIK into the interlayer space of the regenerated HT. Fig. 2 shows the XRD spectra of DIK-Na^+, HT, DIK/Clay and calcined HT. DIK-Na^+ shows sharp peaks indicating a highly crystalline structure (Fig. 2(a)). Pristine HT (Fig. 2(b)) has a strong peak around 11.5° (0.77 nm calculated from Bragg's law); it corresponds to its original basal spacing and this value is in good agreement with supplier's specifications. HT also shows a broad, asymmetric reflection marked

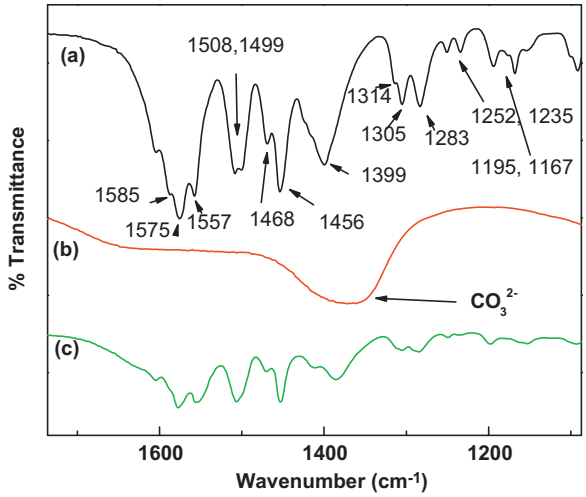

Fig. 1. FTIR spectra of (a) DIK-Na^+, (b) HT, and (c) DIK/Clay.

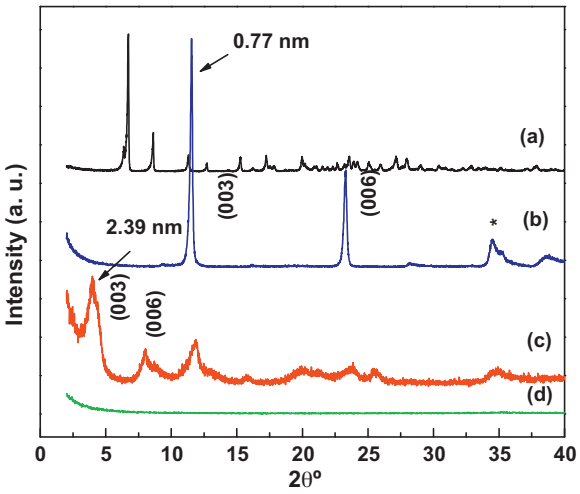

Fig. 2. XRD results of (a) DIK-Na$^+$, (b) HT, (c) DIK/Clay, and (d) CHT.

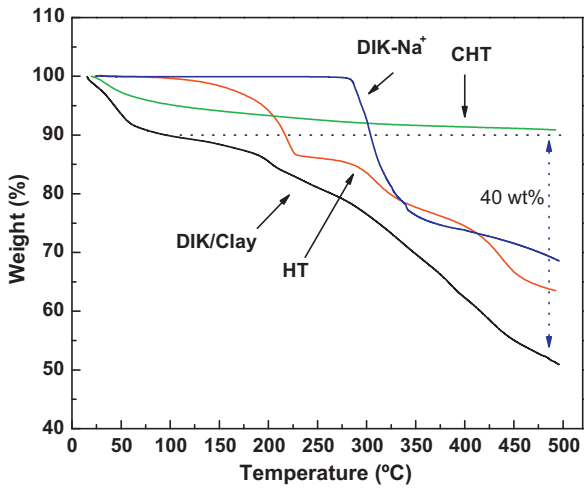

Fig. 3. TGA results of DIK-Na$^+$, clays, and CHT modified with DIK-Na$^+$.

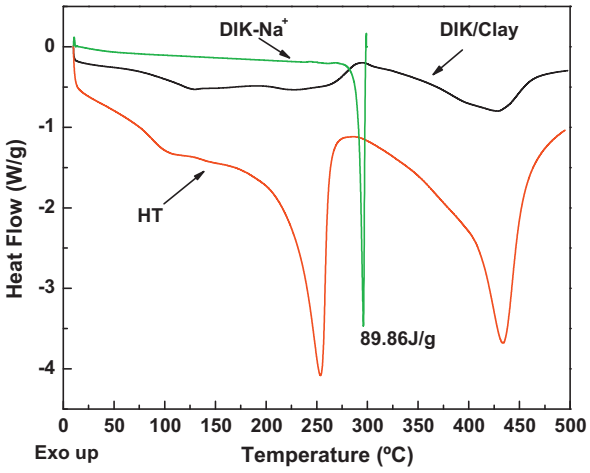

Fig. 4. DSC heating results of DIK-Na$^+$, DIK/Clay, and HT.

as star (*) (Fig. 2(b)) beyond 30°, which may be an indication of turbostratic disorder in the layer stacking (Gago et al., 2004). Calcined HT which lost its crystalline structure due to removal of counter anions by heating does not show any peaks throughout the range from 2° to 40° (Fig. 2(d)). Therefore, based also on the FTIR results, it can be concluded that the carbonate ions are fully removed. Fig. 2, (spectrum (c)), clearly shows the different X-ray peaks of the DIK/Clay as compared to the parent HT (spectrum (b)). It can be shown that the crystalline structure of HT was reformed by regeneration in the presence of DIK-Na$^+$ and peaks corresponding to the regenerated HT have shifted to lower angles. The anionic clay modified with DIK-Na$^+$ shows an angle shifted from 11.5° to 3.9° indicating an increased interlayer space from 0.77 nm to 2.39 nm, and, hence, evidence of intercalation. The broadening of the crystalline reflections in the DIK/Clay represents a loss of HT crystallinity (Costa et al., 2008). Assuming a thickness of 0.45 nm for the Mg–Al double hydroxide layer (Meyn et al., 1990), this result indicates that the interlayer space generated by DIK is 1.94 nm, corresponding to twice the length of the end-to-end distance of DIK. Costantino et al. (2008) and Ambrogi et al. (2002) reported that increased interlayer spacing is responsible for the DIK bilayer presence in the clay interlayer space which is partially interdigitated and perpendicular to the layer plane. It has been reported that the second and the third peaks may correspond to the higher harmonics of the interlayer distance (Tammaro et al., 2007).

3.1.3. Thermal analysis

Fig. 3 shows TGA data of DIK-Na$^+$, HT, CHT, and DIK/Clay. HT shows typically two different weight loss regions. The first region is related to the dehydration of the HT (100–250 °C). The second region (250–527 °C) is responsible for the dehydroxylation and decarbonation reactions (Iyi et al., 2004). DIK-Na$^+$ is thermally stable and starts decomposing around 284 °C, close to its melting point. Since the anions and water of HT were removed, the TGA results of CHT do not show the typical weight losses of HT. The early weight loss of CHT up to 100 °C can be attributed to moisture absorbed during sample preparation. DIK/Clay also does not show a similar pattern of weight loss as compared to the unmodified HT since the original carbonates have been replaced by DIK anions. DIK/Clay shows an early 10 wt% moisture loss and these water molecules may have been absorbed during the DIK-Na$^+$/Clay reaction or the preparation of the sample for the analysis. Subtracting the moisture content of the DIK/Clay, the approximately 40% additional weight loss could be attributed to the weight of both intercalated and coated DIK.

The DSC results of DIK-Na$^+$ show a strong endothermic peak at 291 °C corresponding to its T_m (Fig. 4). HT shows two broad endothermic peaks attributed to the dehydration, and the dehydroxylation and decarbonation reactions (Iyi et al., 2004) discussed in the TGA analysis. However, unlike the unmodified clay, DIK/Clay that does not contain carbonate ions and interlayer water shows very weak broad endothermic peaks. Furthermore, DIK/Clay does not show any T_m, which may suggest an amorphous state for DIK.

3.1.4. Quantitative analysis of DIK/Clay

The DIK loading of DIK/Clay was determined by carbon and nitrogen elemental analysis (Table 1). Carbon and nitrogen are unique elements present only in the DIK and not in the CHT. Calculated DIK loadings on the modified clays based on carbon and nitrogen are 40.0% and 41.3%, respectively. Therefore, it may be

Table 1
Elemental analysis of clays, API and their combinations.

Material	% Carbon	% Nitrogen
HT[a]	4.0	0.0
CHT[a]	0.0	0.0
DIK[a]	56.7	4.7
DIK/Clay[b]	22.7	1.9

[a] Calculated.
[b] Experimental.

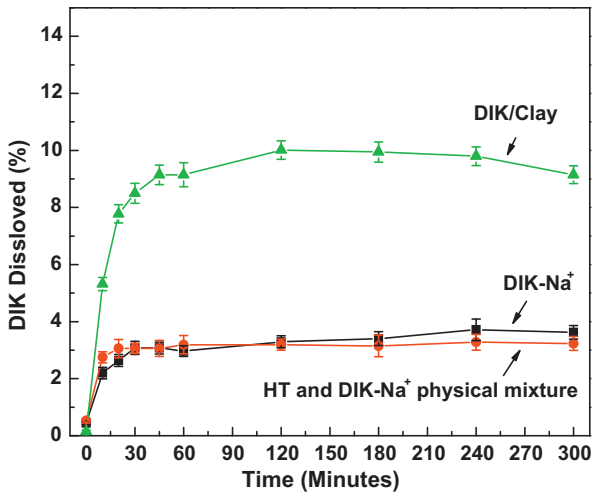

Fig. 5. Dissolution results in simulated gastric fluid (pH 1.2) of DIK-Na^+, DIK/Clay (containing approximately 40% DIK) and a HT/DIK-Na^+ physical mixture containing 40% DIK-Na^+.

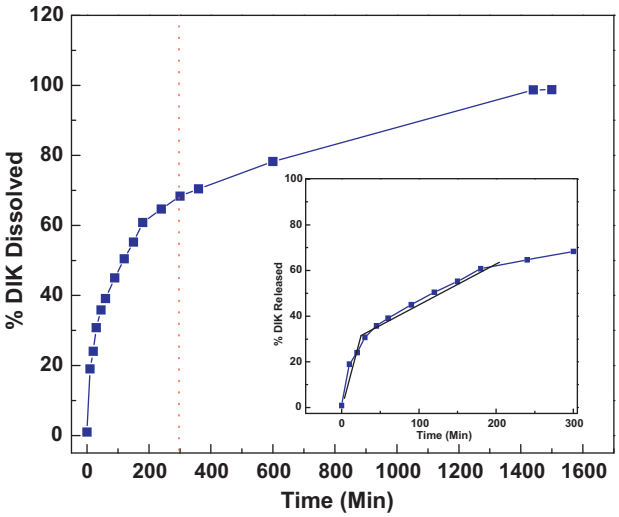

Fig. 6. Dissolution profiles of DIK/Clay in simulated body fluid (phosphate buffer solution, pH 7.4).

assumed that approximately 40% of the DIK was loaded on the clay matrix. This is in reasonable agreement with the results of Ambrogi et al. (2002) who, by using a different type of HT and a different preparation method, reported that roughly 50 wt% DIK was intercalated.

3.1.5. Dissolution tests at different pH

Fig. 5 shows the percentage of the dissolved DIK from DIK-Na^+, DIK-Na^+/HT physical mixture and DIK/Clay as a function of time in acidic buffer. DIK-Na^+ rapidly dissolves in neutral pH water. However, as mentioned earlier, its solubility is dramatically decreased at lower pH. Fig. 5 shows that less than 4% DIK is dissolved from both DIK-Na^+ and from the physical mixture of DIK-Na^+ and HT while less than 10% DIK was dissolved from DIK/Clay in the simulated gastric fluid (SGF) at pH 1.2. Therefore, it is shown that HT does not affect the dissolution behavior of DIK-Na^+. The increased apparent solubility of DIK from the DIK/Clay can be explained by the following considerations:

1. DIK released in its molecular form (non-ionized) while HT dissolved rapidly under the acidic conditions. (Del Arco et al., 2008).
2. Amorphous-like state of DIK in the anionic clay interlayer space.
3. Increased wettability of DIK associated with the anionic nanoclay (McGinity and Lach, 1977).

It is to be noted that clays can increase, not only the apparent solubility, but also the API release rate due to their hydrophilic and swelling properties in aqueous solution (McGinity and Harris, 1980). Initially, it was expected that DIK/Clay may achieve a sustained DIK release. However, since HT was dissolved at the low pH medium within 30 min sustained DIK release was not observed.

The acidic solution firstly dissolves HT to produce a mixture of $MgCl_2$ and $AlCl_3$ and converts DIK anions into an acid form; the amorphous-like DIK is then exposed to the medium simultaneously. According to the Noyes-Whitney equation (Noyes and Whitney, 1897; Wurster and Taylor, 1965), the dissolution rate, among other parameters, is proportional to the total area of the DIK exposed to the dissolution medium. Therefore, it is not surprising that DIK/Clay shows the highest dissolution rate (Fig. 5) since, assuming that DIK is in an amorphous state, it is spread over a larger area in the clay interlayer space. It should be noted that the possibility of inappropriate sampling and poor detection may exist as a result of precipitation of the protonated DIK at the bottom of the cell, although increase in the agitation speed and allowable time up to 24 h did not appear to change the maximum amount of API dissolved. A total recovery experiment performed by filtering the buffer medium and dissolving up in a base would possibly confirm if greater amounts of DIK are actually present.

Fig. 6 shows the dissolution profile of DIK/Clay in SBF at a 7.4 pH. Since HT does not dissolve in the neutral pH medium, the intercalated DIK anions had to be ion exchanged with the phosphate ions of the medium in order to diffuse out from the clay interlayer (Ambrogi et al., 2002). Since this procedure takes time, DIK could be released slowly. However, the DIK release rate at an early stage up to 30 min was somewhat faster (dissolution rate: 1.03%/min) than the release after 30 min. This could provide evidence that DIK is, not only intercalated in the interlayer space, but is also coating the outside clay surface. Unlike DIK at the interlayer, the DIK at the outside layers will be exposed directly to the medium and will be dissolved immediately.

After 30 min and up to 240 min, the release rate of DIK slowed down indicating that release from the clay interlayer was dominant (dissolution rate: 0.15%/min). Based on Fig. 6, a rough approximation of the concentration of DIK on the clay surface is 30 wt%. After 240 min, the dissolution of DIK/Clay is the slowest. This may be due to the precipitated DIK/Clay being stacked at the bottom of the vessel, even at an agitation speed of 50 rpm, and the inner stacked DIK/Clay was not directly exposed to the medium making diffusion slower. It is shown that DIK/Clay achieved 100% DIK release after 25 h. This suggests that the dissolution method can be another method for calculating DIK loading on the clay along with the elemental analysis. Note that Fig. 6 is very similar to Fig. 7, obtained with different clay and different experimental conditions, in the article by Ambrogi et al. (2002).

3.1.6. Mechanisms of DIK release from DIK/Clay at different pH

API release rates are usually explained by three controlling mechanisms, namely diffusion, swelling and erosion (Yang et al., 2010; Langer and Peppas, 1983). Among others, two simple, semi-empirical equations, the Korsmeyer–Peppas (power law) (Korsmeyer et al., 1983) and the equation developed by Peppas and Sahlin (Siepmann and Peppas, 2001; Peppas and Sahlin, 1989), can be used to describe the API release behavior from a matrix.

The Korsmeyer–Peppas (power law) equation is:

$$\frac{M_t}{M_\infty} = kt^n \quad (1)$$

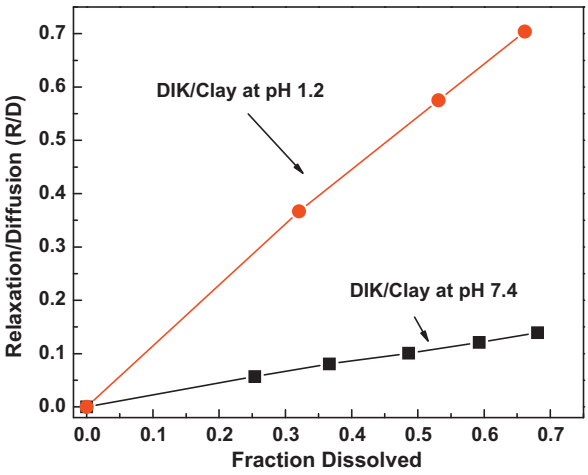

Fig. 7. *R/D* ratio values vs. API fraction dissolved for the DIK/Clay system at different pH of 1.2 and 7.4.

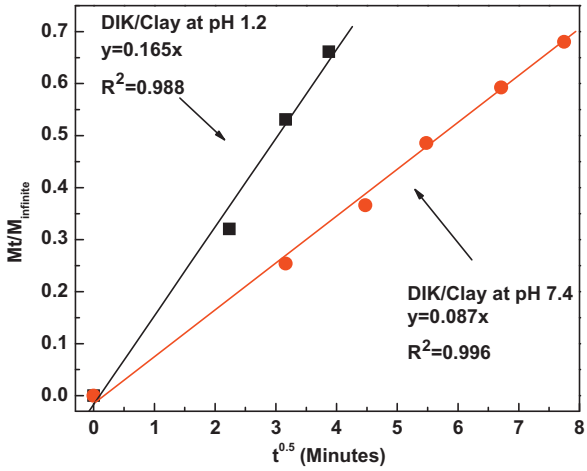

Fig. 8. DIK release from DIK/Clay as a function of time$^{0.5}$, (■) DIK/Clay at pH 1.2 and (●) DIK/Clay at pH 7.4.

where M_t and M_∞ are the absolute cumulative amounts of API released at time t and infinite time, respectively, "k" is a constant incorporating structural and geometric characteristics of the sample, and "n" is the release kinetics exponent. This "n" value is used in order to differentiate between release mechanisms. The interpretation of "n" value for different diffusion mechanisms is given in Table 2.

The heuristic equation developed by Peppas and Sahlin (1989) can be used to estimate the effect of API diffusion and polymer erosion on the anomalous transport:

$$\frac{M_t}{M_\infty} = k_1 t^m + k_2 t^{2m} \quad (2)$$

where "k_1", "k_2" and "m" are constants. The first term on the right hand side represents the Fickian diffusional contribution (D), whereas the second term represents the polymer relaxation contribution (R). "m" is geometrical factor (in this case $m = 0.5$: disk or film). Eqs. (1) and (2) are valid only up to 60% dissolution ($M_t/M_\infty < 0.6$) (Costa and Sousa Lobo, 2001). The ratio of relaxation (R) and diffusion (D) contributions (Peppas and Sahlin, 1989; Bettini et al., 1994) could be calculated as:

$$\frac{R}{D} = \frac{k_2 t^m}{k_1} \quad (3)$$

Table 3 shows results calculated from Eqs. (1) and (2). The exponent for Eq. (1) indicates that both systems exhibit anomalous transport.

Table 2
Interpretation of diffusional release mechanisms from polymeric films (Costa and Sousa Lobo, 2001).

Release exponent (n)	Drug transport mechanism	Rate as a function of time
0.5	Fickian diffusion (diffusion dominant)	$t^{-0.5}$
$0.5 < n < 1.0$	Anomalous transport (non Fickian diffusion)	t^{n-1}
1.0	Case-II transport[a] (erosion dominant)	Zero order release
$n > 1.0$	Super Case-II transport[b]	t^{n-1}

[a] Case II transport (Case II relaxational release) is the drug transport mechanism associated with stresses and state-transition in hydrophilic glassy polymers which swell or erode in water or biological fluids (non-Fickian) (Peppas and Sahlin, 1989; Hassan and Durning, 1999).

[b] Super case-II transport is indicating API release due to the combination of API diffusion and polymer relaxation/dissolution as opposed to simple Fickian diffusion (Rathbone et al., 2003).

Since the DIK/Clay dissolved very quickly in SGF within 30 min, it was anticipated that the erosion mechanism would be dominant. From the k_1 and k_2 values of Table 3 obtained by regression, the R/D ratio can be calculated (Eq. (3)) and plotted vs. fraction dissolved in Fig. 7. The results show that for both pH values diffusion dominates over relaxation. However, the R/D ratios in the pH 7.4 solution are much lower than the ones in the pH 1.2 solution since the clay did not dissolve in the pH 7.4 buffer solution but was able to exchange slowly DIK anions for buffer anions.

Since both DIK/Clay dissolution profiles from pH 1.2 and 7.4 have a stronger diffusion than relaxation component, dissolution data were fitted to the Fickian model (no erosion) presented earlier which describes API diffusion from a disc:

$$\frac{M_t}{M_\infty} = 4\sqrt{\frac{D_{app} t}{L^2 \pi}} \quad (4)$$

where L is the disk thickness, initially the same for all samples, D_{app} is the apparent diffusion coefficient depending only on the molecular size of the API and the temperature of release (Bhaskar et al., 1986; Cypes et al., 2003). Fig. 8 shows dissolution profiles of DIK from DIK/Clay at different pH fitted to the Fickian model. DIK release from DIK/Clay at pH 7.4 has a larger R^2 value than at pH 1.2 since no erosion occurs in this case.

3.2. DIK-functionalized nanoclay/Eudragit® E100 composites

A DIK/Clay hybrid was shown to improve DIK apparent solubility due to the amorphous state of the DIK in the clay interlayer space. Therefore, it was anticipated that incorporation of the nanoclay hybrid may also increase the apparent solubility of the DIK released from the hybrid/polymer composites.

3.2.1. XRD analysis

Eudragit® E100 is an amorphous polymer showing no crystalline peaks in its XRD spectrum (Fig. 9(a)). However, Eudragit® E100 mixed with 15 wt% DIK-Na$^+$ shows a major peak at 6.67° (Fig. 9(b)) and other minor peaks elsewhere. These peaks provide evidence that DIK-Na$^+$ is not dissolved during melt mixing but dispersed as crystalline particles. Eudragit® E100 compounded with DIK/Clay (10 wt%) (Fig. 9(c)) also shows crystalline peaks but these are not exactly the same as the ones of Eudragit® E100 compounded with DIK-Na$^+$ but more closely correspond to those of the nanoclay hybrid DIK/Clay (Fig. 9(d)). This suggests that the DIK in the clay interlayer space did not undergo any changes during the melt mixing process. This is because the first peak in Fig. 9(d) marked with a

Table 3
Dissolution fitting results of DIK/Clay in media of different pH.

System	Power law (Eq. (1)), $(M_t/M_\infty) = kt^n$	Peppas and Sahlin (Eq. (2)), $(M_t/M_\infty) = k_1 t^{0.5} + k_2 t$	
	n ±95% CI	k_1 ($min^{-0.5}$) ±95% CI	k_2 (min^{-1}) ±95% CI
DIK/Clay at pH 1.2	0.64 ± 0.05	0.11 ± 0.02	0.02 ± 0.01
DIK/Clay at pH 7.4	0.54 ± 0.04	7.78 ± 0.17	0.14 ± 0.01

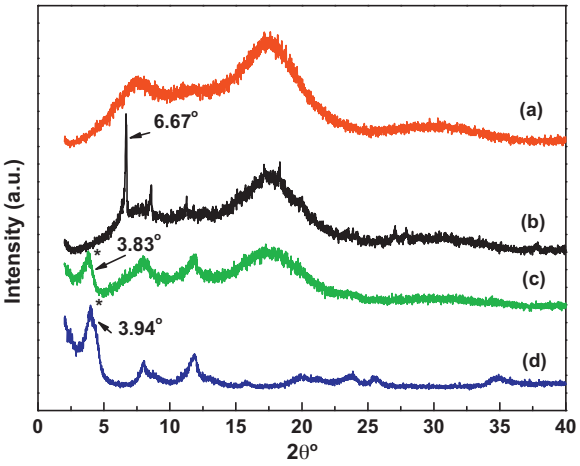

Fig. 9. XRD results of (a) Eudragit® E100, (b) Eudragit® E100/15 wt% DIK-Na^+, (c) Eudragit® E100–10 wt% DIK/Clay, and (d) DIK/Clay (samples prepared in batch mixer).

star corresponding to the intercalated DIK, does not shift to a higher 2θ angle but to a slightly lower 3.83°2θ angle in Fig. 9(c). The slightly increased basal spacing of DIK/Clay in the Eudragit® E100 matrix after hot melt processing may have resulted from a small amount of polymer that migrated into the anionic clay interlayer space during melt compounding. Similar effects have been observed in other studies on nanoclay composites (Ha and Xanthos, 2009; Kawasumi et al., 1997).

3.2.2. SEM and EDX analysis

The fracture surfaces of Eudragit® E100 and its melt mixed compounds were examined by SEM. Eudragit® E100 compounded with DIK-Na^+ shows agglomerated crystalline particles (Fig. 10 (top)). DIK/Clay hybrid particles shown in Fig. 10 (bottom) are significantly smaller as compared to DIK-Na^+ particles and are more uniformly dispersed (average particle size 10 μm vs. 30 μm).

3.2.3. Dissolution test

The data from the dissolution tests in SGF of Eudragit® E100 compounded with DIK-Na^+, DIK/Clay and physically mixed with DIK-Na^+ are shown in Fig. 11.

The improved apparent solubility of DIK-Na^+ from Eudragit® E100/DIK-Na^+ compounds as compared to DIK-Na^+ from the Eudragit® E100/DIK-Na^+ physical mixture may be attributed to the less aggregated DIK-Na^+ particles in the matrix after hot melt mixing and the enhanced wettability due to the polymeric excipient. The DIK from the physical mixture was separated from the polymer powder and floated as segregated particles when the sample was immersed into the medium. As a result, the hydrophobic DIK (at low pH) tended to minimize its contacting surface with the medium, thereby reducing wettability. The DIK from the Eudragit® E100–DIK/Clay composite shows roughly 10% increased solubility

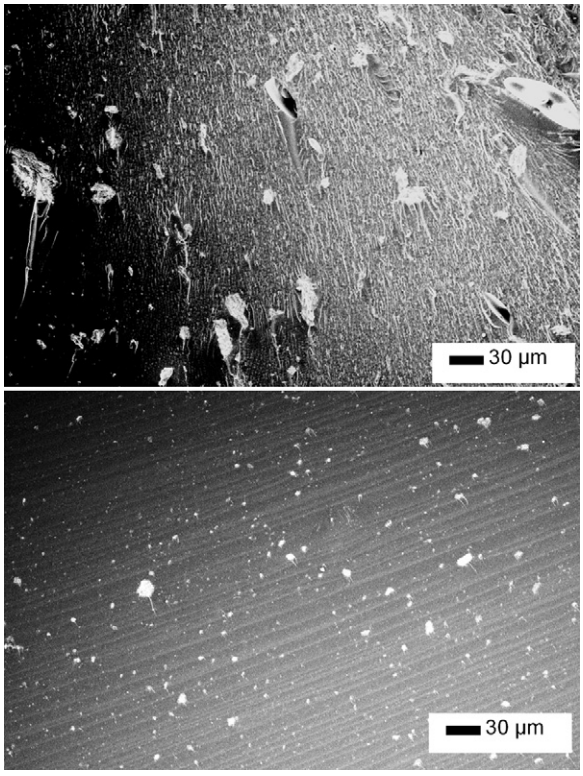

Fig. 10. SEM images of fracture surface of (top) Eudragit® E100/4 wt% DIK-Na^+ and (bottom) Eudragit® E100–10 wt% DIK/Clay (samples prepared in batch mixer).

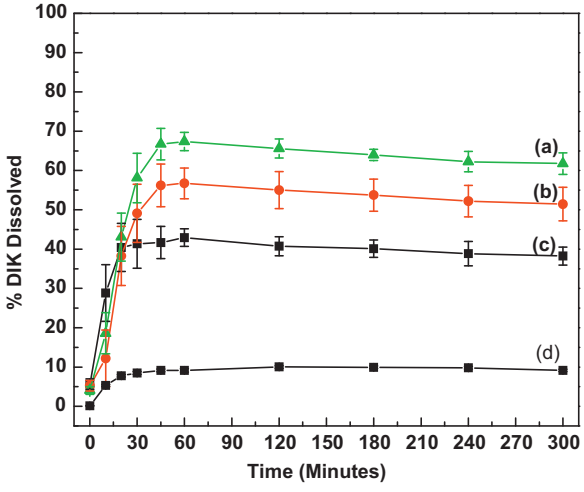

Fig. 11. Dissolution results in SGF (pH 1.2) of: (a) Eudragit® E100–10 wt% DIK/Clay, (b) Eudragit® E100/4 wt% DIK-Na^+, (c) physical mixture of Eudragit® E100 and 4 wt% DIK-Na^+ (samples prepared by batch mixer) (*Note*: Data on DIK/Clay (d) added for comparison).

as compared to the DIK from the Eudragit® E100/DIK-Na$^+$ compound. This increased apparent solubility may be attributed to the following:

1. The crystalline DIK-Na$^+$ is at least partially present in an amorphous state in the anionic clay interlayer space and would therefore dissolve more efficiently in the medium.
2. The smaller size of the DIK/Clay as compared to the DIK-Na$^+$ agglomerates in the matrix would provide a larger contacting surface area, thereby affecting rate of dissolution and apparent solubility.

Along with the increased apparent solubility, it should be noted that the DIK dissolution results from Eudragit® E100–DIK/Clay have a relatively lower variability as compared to those from the Eudragit® E100/DIK-Na$^+$ compound due to the smaller and more uniformly dispersed DIK/Clay particles. However, the apparent solubility cannot reach 100%, unlike the one in the case of miscible API-polymer systems (Liu et al., 2009) which confirms again that fully dissolved amorphous API in the polymer matrix is desirable in order to achieve the maximum apparent solubility.

The DIK dissolution rates from the Eudragit® E100 compounds that contain either only DIK or the nanoclay hybrid do not show significantly differences. This could be evidence that the surfactant effect of Eudragit® E100 in the earlier stages of the dissolution test was dominant and it prevailed over the effect of the clay hybrid. The physical mixture shows a slightly higher dissolution rate at the early stages. This is because the small size Eudragit® E100 powder (other samples were pressed to thin disks) dissolved faster and affected immediately the overall mixture dissolution rate.

3.3. Eudragit® S100-plasticizer compounds with DIK/Clay

The quaternary system (polymer/plasticizer/DIK/Clay) for this particular combination employs a different acrylic polymer and its intended application is sustained DIK delivery.

3.3.1. Thermal analysis

Fig. 12 contains glass transition temperature values for Eudragit® S100 plasticized with 20% TEC and the blends/composites of the plasticized mixture with DIK-Na$^+$ and DIK/Clay. The glass transition temperature of composite (e) containing plasticizer and DIK/Clay was somewhat higher than that of Eudragit® S100 containing either only plasticizer (b) or plasticizer and DIK-Na$^+$ (c or d). This increased T_g is a common phenomenon in clay composites since the dispersed clay restricts the mobility of the polymer chains (Uhl et al., 2004). It can also be argued that during melt processing the DIK, which could also be acting as a plasticizer, was not released from the interlayer. Ha and Xanthos (2010) reported that ionic liquids, which could be functioning as plasticizers, exerted only a small plasticizing effect on PLA due to the barrier effect of the nanoclay layers.

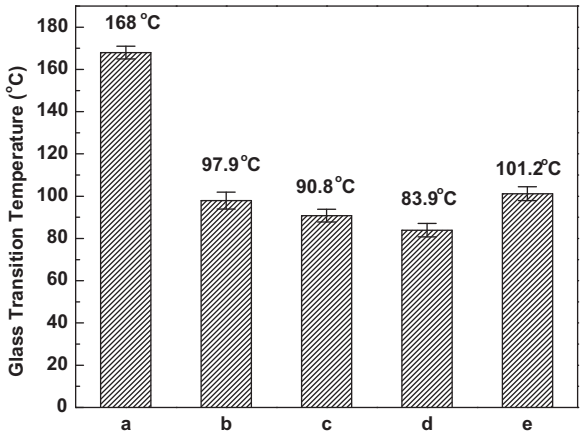

Fig. 12. T_g of Eudragit® S100 composites of (a) Eudragit® S100, (b) Eudragit® S100/20 wt% TEC, (c) Eudragit® S100/20 wt% TEC–4 wt% DIK-Na$^+$, (d) Eudragit® S100/20 wt% TEC–15 wt% DIK-Na$^+$, and (e) Eudragit® S100/20 wt% TEC–10 wt% DIK/Clay (samples prepared in batch mixer).

3.3.2. SEM and EDX analysis

Fig. 13 shows a fracture surface of the Eudragit® S100 composite containing 20 wt% TEC and 10 wt% DIK/Clay. By rough approximation based on the SEM images, the DIK/Clay particles are smaller than 5 μm (Figs. 13 and 14) and the particles are more uniformly dispersed than in the Eudragit® E100 matrix (Fig. 10 (bottom)). This suggests that Eudragit® S100 has better compatibility with DIK/Clay than Eudragit® E100.

EDX mapping (Fig. 14) was carried out in order to identify the location of DIK/Clay in the matrix and the degree of dispersion of the hybrid. The shape and location of the DIK/Clay could be identified by EDX mapping of Mg, Al, and Cl since HT contains magnesium and aluminum, and DIK contains chlorine. On the EDX images, dense bright dots indicate higher population of each individual element. The population of chlorine matched with magnesium and aluminum indicates that DIK is still associated with the nanoclay after mixing.

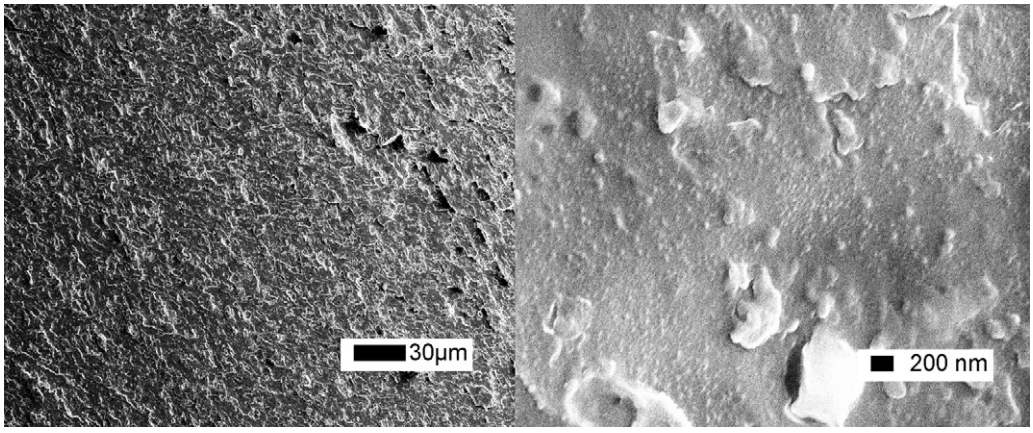

Fig. 13. SEM image of Eudragit® S100/20 wt% TEC–10 wt% DIK/Clay fracture surface.

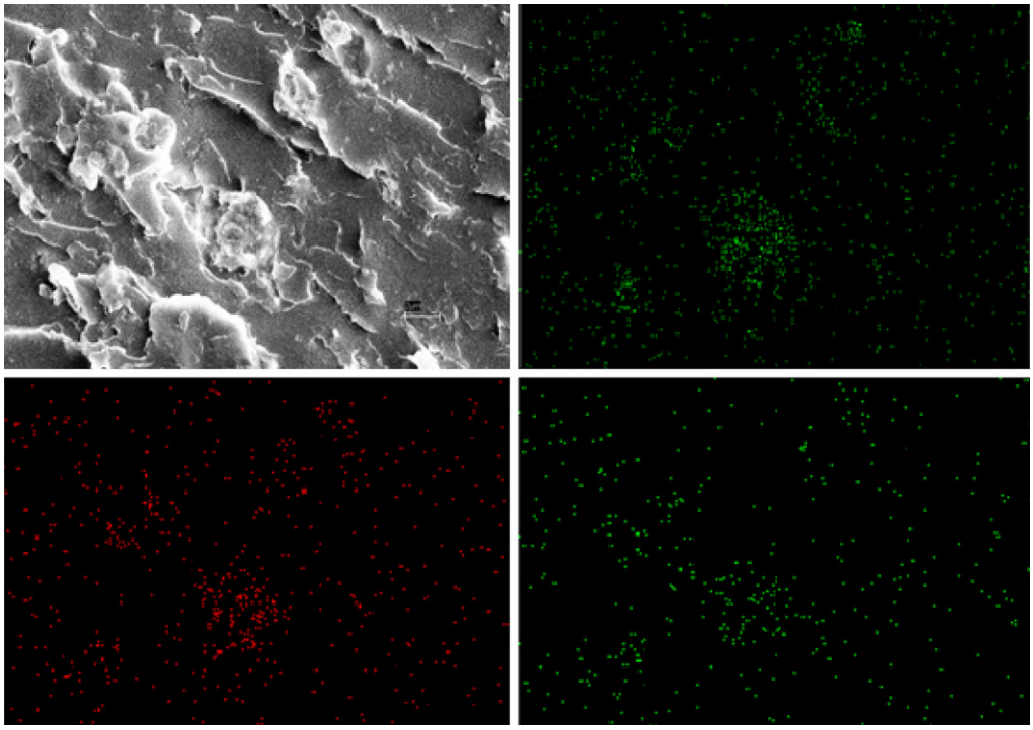

Fig. 14. Images of Eudragit® S100/20 wt% TEC–10 wt% DIK/Clay by: (a) SEM, (b) EDX Mg mapping, (c) EDX Al mapping, and (d) EDX Cl mapping (samples prepared in batch mixer).

3.3.3. Dissolution study

In the SGF acidic medium at pH 1.2, the anionic nanoclay was dissolved shortly after its immersion into the medium and the DIK in the clay interlayer would, thus, be immediately released. On the other hand, since HT is not soluble at a pH 7.4 SBF medium, sustained DIK release would be expected. Fig. 15 shows the dissolution profiles of Eudragit® S100/20 wt% TEC containing 4 wt% DIK-Na^+ and 10 wt% DIK/Clay. Eudragit® S100 containing the DIK shows a relatively slow release profile while the one containing DIK/Clay shows an even slower DIK release. The different release behavior between the two compounds can be explained as follows:

1. DIK in the clay interspacing may experience one more step in its release path, which is diffusion from the clay interlayer space.
2. Nanoclay platelets may act as barriers and slow down the DIK release process in the polymer matrix and/or its buffer solution.

Note that Eudragit® S100/20 wt% TEC containing 10 wt% DIK/Clay achieved almost 100% DIK release, while DIK/Clay in Eudragit® E100 reached only 70% (Fig. 11). This different apparent solubility is mainly due to the different water solubility of the DIK in the different pH media.

Dissolution results of Eudragit® S100 compounds were fitted with Eqs. (1) and (2) (ordinary least square regression, ±95% confidence limits) and results are listed in Table 4. It is to be noted that Eudragit® S100 compounds containing DIK/Clay have a larger

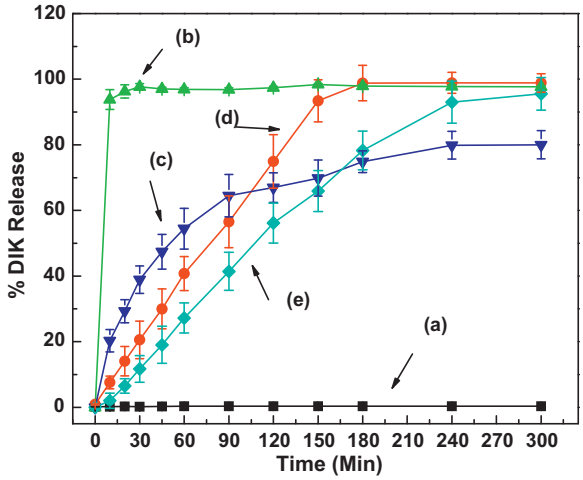

Fig. 15. API dissolution results in pH 7.4 buffer of: (a) Eudragit® S100, (b) DIK-Na^+, (c) DIK/Clay, (d) Eudragit® S100/20 wt% TEC–4 wt% DIK-Na^+ and (e) Eudragit® S100/20 wt% TEC–10 wt% DIK/Clay (samples prepared in batch mixer).

"*n*" exponent value (Eq. (1)) as compared to the ones that do not contain clay. This could be an indication that the diffusion tendency of DIK vs. erosion was reduced due to the presence of the clay in the polymer matrix. Values calculated by Eq. (2) also show

Table 4
DIK dissolution fitting results (pH 7.4) from Eudragit® S100/TEC matrix as per Eqs. (1) and (2).

Sample	Power law (Eq. (1)) $(M_t/M_\infty) = kt^n$	Peppas and Sahlin (Eq. (2)) $(M_t/M_\infty) = k_1 t^{0.5} + k_2 t$	
	n ±95% CI	k_1 ($min^{-0.5}$) ±95% CI	k_2 (min^{-1}) ±95% CI
Eudragit® S100/20 wt% TEC–4 wt% DIK-Na^+	0.75 ± 0.02	0.75 ± 0.01	0.56 ± 0.05
Eudragit® S100/20 wt% TEC–10 wt% DIK/Clay	0.92 ± 0.03	0.02 ± 0.01	0.57 ± 0.04

interesting results in that the sample containing nanoclay showed reduced diffusion constant while the erosion constant remains at a similar value as compared to the sample without the nanoclay. Therefore, it can be interpreted that DIK release from the polymer matrix was either obstructed in the presence of nanoclay due to the barrier property of the latter, or the actual release mechanism was modified in the presence of the nanoclay.

4. Conclusions

An anionic nanoclay HT was successfully intercalated by DIK at about 40 wt% loading. DIK/Clay showed increased interlayer spacing and less tendency to agglomeration vs. the unmodified clay. DIK released from DIK/Clay showed not only increased apparent solubility and dissolution rate than DIK-Na^+ in SGF but also sustained DIK release in SBF. Increased solubility and dissolution rate in SGF might be due to: (a) non ionized form of DIK and rapid dissolution of HT, (b) the amorphous state of DIK in the clay interlayer space and (c) increased wettabililty. Sustained DIK release from DIK/Clay in SBF can also be an indication of intercalated DIK, whereas fast release at the initial stages may be due to the presence of DIK coating on the clay. The Korsmeyer–Peppas (Power law) and the Peppas and Sahlin equations predicted the DIK dissolution mechanism from the nanoclay. DIK dissolution from the modified clay in different pH media showed that diffusion was the dominant mechanism although its magnitude differed among the two different pH buffers used. DIK dissolution from the clay showed a good fitting with Fickian diffusion.

Ternary polymer systems containing DIK modified nanoclay were compared with binary systems in which DIK was melt mixed with the polymer directly. Ternary systems showed several advantages. For example, the DIK from Eudragit® E100 melt mixed with DIK/Clay had higher DIK apparent solubility than from a binary system, and less dissolution variation. However, use of this ternary system could not increase the DIK apparent solubility as much as DIK-polymer miscible system did. As an example, Eudragit® E100 containing IND/Clay showed less apparent IND solubility than Eudragit® E100/IND system (Ha, 2011). Eudragit® S100 compounds containing plasticizer and DIK/Clay showed slower DIK release than in the absence of clay in pH 7.4 buffer solution. This slower release behavior due to the presence of the nanoclay platelets in the polymer matrix would be related to the formation of a more tortuous DIK diffusion path and/or modification of the release mechanism in the presence of the nanoclay. It remains to be seen whether a system containing fully exfoliated nanoclay and DIK separately mixed with the polymer would have different dissolution characteristic than the present system.

Acknowledgement

The research in this article is supported by the US National Science Foundation under GOALI Grant No. 0927142.

References

Aguzzi, C., Cerezo, P., Viseras, C., Caramella, C., 2007. Use of clays as drug delivery systems: possibilities and limitations. Appl. Clay Sci. 36, 22–36.

Ambrogi, V., Fardella, G., Grandolini, G., Perioli, L., Tiralti, M.C., 2002. Intercalation compounds of hydrotalcite-like anionic clays with anti-inflammatory agents, II: Uptake of diclofenac for a controlled release formulation. AAPS PharmSciTech 3, 1–6.

Bettini, R., Colombo, P., Massimo, G., Catellani, P.L., Vitali, T., 1994. Swelling and drug release in hydrogel matrices: polymer viscosity and matrix porosity effects. Eur. J. Pharm. Sci. 2, 213–219.

Bhaskar, R., Murthy, R.S.R., Miglani, B.D., Viswanathan, K., 1986. Novel method to evaluate diffusion controlled release of drug from resinate. Int. J. Pharm. 28, 59–66.

Bugatti, V., Costantino, U., Gorrasi, G., Nocchetti, M., Tammaro, L., Vittoria, V., 2010. Nano-hybrids incorporation into poly(ε-caprolactone) for multifunctional applications: mechanical and barrier properties. Eur. Polym. J. 46, 418–427.

Budavari, S., O'Neil, M.J., Smith, A., Heckelman, P.E., Kinneary, J.F., 1996. The Merck Index, 12th ed. Merck & Co., Inc., Whitehouse Station, NJ.

Campbell, K., Craig, D.Q.M., McNally, T., 2008. Poly(ethylene glycol) layered silicate nanocomposites for retarded drug release prepared by hot-melt extrusion. Int. J. Pharm. 363, 126–131.

Colthup, N.B., Daly, L.H., Wiberley, S.E., 1975. Introduction to Infrared and Raman Spectroscopy, 2nd ed. Academic Press Inc., New York, NY.

Costa, F.R., Leuteritz, A., Wagenknecht, U., Jehnichen, D., Häußler, L., Heinrich, G., 2008. Intercalation of Mg–Al layered double hydroxide by anionic surfactants: preparation and characterization. Appl. Clay Sci. 38, 153–164.

Costa, P., Sousa Lobo, J.M., 2001. Modeling and comparison of dissolution profiles. Eur. J. Pharm. Sci. 13, 123–133.

Costantino, U., Ambrogi, V., Nocchetti, M., Perioli, L., 2008. Hydrotalcite-like compounds: Versatile layered hosts of molecular anions with biological activity. Microporous and Mesoporous Materials 107, 149–160.

Crowley, M.M., Fredersdorf, A., Schroeder, B., Ucera, S., Prodduturi, S., Repka, M.A., 2004. The influence of guaifenesin and ketoprofen on the properties of hot-melt extruded polyehylene oxide films. Eur. J. Pharm. Sci. 22, 409–418.

Cypes, S.H., Saltzman, W.M., Giannelis, E.P., 2003. Organosilicate-polymer drug delivery systems: controlled release and enhanced mechanical properties. J. Control. Release 90, 163–169.

Del Arco, M., Fernandez, A., Martin, C., Sayalero, M.L., Rives, V., 2008. Solubility and release of fenamates intercalated in layered double hydroxides. Clay Miner. 43, 255–265.

Del Arco, M., Cebadera, E., Gutierrez, S., Martin, C., Montero, M.J., Rives, V., Rocha, J., Sevilla, M.A., 2004. Mg–Al layered double hydroxides with intercalated indomethacin: synthesis, characterization, and pharmacological study. J. Pharm. Sci. 93, 1649–1658.

Dong, Y., Feng, S.-S., 2005. Poly(D,L-lactide-co-glycolide)/montmorillonite nanoparticles for oral delivery of anticancer drugs. Biomaterials 26, 6068–6076.

Gago, S., Pillinger, M., Valente, A.A., Santos, T.M., Rocha, J., Goncalves, I.S., 2004. Immobilization of oxomolybdenum species in a layered double hydroxide pillared by 2,2′-bipyridine-5,5′-dicarboxylate anions. Inorg. Chem. 43, 5422–5431.

Guarino, A., Bisceglia, M., Castellucci, G., Iacono, G., Casali, L.G., Bruzzese, E., Musetta, A., Greco, L., 2001. Smectite in the treatment of acute diarrhea: a nationwide randomized controlled study of the Italian society of pediatric gastroenterology and hepatology (SIGEP) in collaboration with primary care pediatricians. J. Pediatr. Gastr. Nutr. 32, 71–75.

Ha, J.U., 2011 Study of controlled release of active pharmaceutical ingredients from functionalized nanoclays and polymer matrices. Ph.D. Dissertation. New Jersey Institute of Technology, Newark, NJ 07102.

Ha, J.U., Xanthos, M., 2009. Functionalization of nanoclays with ionic liquids for polypropylene composites. Polym. Compos. 30, 534–542.

Ha, J.U., Xanthos, M., 2010. Novel modifiers for layered double hydroxides and their effects on the properties of polylactic acid composites. Appl. Clay Sci. 47, 303–310.

Hassan, M.M., Durning, C.J., 1999. Effects of polymer molecular weight and temperature on case II transport. J. Polym. Sci. Polym. Phys. 37, 3159–3171.

Iyi, N., Matsumoto, T., Kaneko, Y., Kitamura, K., 2004. Deintercalation of carbonate ions from a hydrotalcite-like compound: enhanced decarbonation using acidic salt mixed solution. Chem. Mater. 16, 2926–2932.

Kamena, K., 2010. Nanoclays and their emerging markets. In: Xanthos, M. (Ed.), Functional Fillers for Plastics. , 2nd ed. Wiley-VCH Verlag GmbH & Co., Weinheim, Germany, pp. 177–188.

Kawasumi, M., Hasegawa, N., Kato, M., Usuki, A., Okada, A., 1997. Preparation and mechanical properties of polypropylene–clay hybrids. Macromolecules 30, 6333–6338.

Kincl, M., Meleh, M., Veber, M., Vrecer, F., 2004. Study of physicochemical parameters affecting the release of diclofenac sodium from lipophilic matrix tablets. Acta Chim. Slov. 51, 409–425.

Korsmeyer, R.W., Gurny, R., Buri, E.M., Peppas, N.A., 1983. Mechanism of solute release from porous hydrophilic polymer. Int. J. Pharm. 15, 25–35.

Langer, R., Peppas, N., 1983. Chemical and physical structure of polymers as carriers for controlled release of bioactive agents: a review. Polym. Rev. 23, 61–126.

Li, B., He, J.G., Evans, D., Duan, X., 2004a. Inorganic layered double hydroxides as a drug delivery system—intercalation and in vitro release of fenbufen. Appl. Clay Sci. 27, 199–207.

Li, B., He, J., Evans, D.G., Duan, X., 2004b. Enteric-coated layered double hydroxides as a controlled release drug delivery system. Int. J. Pharm. 287, 89–95.

Linares, C.F., Brikgi, M., 2006. Interaction between antimicrobial drugs and antacid based on cancrinite-type zeolite. Micropor. Mesopor. Mater. 96, 141–148.

Liu, H., Wang, P., Zhang, X., Shen, F., Gogos, C.G., 2009. Effects of extrusion process parameters on the dissolution behavior of indomethacin in Eudragit® E PO solid dispersions. Int. J. Pharm. 383, 161–169.

McGinity, J.W., Lach, J.L., 1977. Sustained release applications of montmorillonite interaction with amphetamine sulfate. J. Pharm. Sci. 66, 63–66.

McGinity, J.W., Harris, M.R., 1980. Increasing dissolution rates of poorly soluble drugs by adsorption to montmorillonite. Drug Dev. Ind. Pharm. 6, 35–48.

Meyn, M., Beneke, K., Lagaly, G., 1990. Anion-exchange reactions of layered double hydroxides. Inorg. Chem. 29, 5201–5207.

Nollenberger, K., Gryczke, A., Meier, C., Dressman, J., Schmidt, M.U., Brühne, S., 2009. Pair distribution function X-ray analysis explains dissolution characteristics of felodipine melt extrusion products. J. Pharm. Sci. 98, 1476–1486.

Noyes, A.A., Whitney, W.R., 1897. The rate of solution of solid substances in their own solutions. J. Am. Chem. Soc. 19, 930–934.
Park, J.K., Choy, Y.B., Oh, J.-M., Kim, J.Y., Hwang, S.-J., Choy, J.-H., 2008. Controlled release of donepezil intercalated in smectite clays. Int. J. Pharm. 359, 198–204.
Peppas, N.A., Sahlin, J.J., 1989. A simple equation for the description of solute release. III. Coupling of diffusion and relaxation. Int. J. Pharm. 57, 169–172.
Rathbone, M.J., Hadgraft, J., Roberts, M.S., 2003. Modified Release Drug Delivery Technology. Marcel Dekker, Inc., New York, NY.
Schilling, S.U., Shah, N.H., Waseem Malick, A., McGinity, J.W., 2010. Properties of melt extruded enteric matrix pellets. Eur. J. Pharm. Biopharm. 74, 352–361.
Schmidt, D., Shah, D., Giannelis, E.P., 2002. New advances in polymer layered silicate nanocomposites. Curr. Opin. Solid State Mater. 6, 205–212.
Siepmann, J., Peppas, N.A., 2001. Modeling of drug release from delivery systems based on hydroxypropyl methylcellulose (HPMC). Adv. Drug Deliv. Rev. 48, 139–157.
Six, K., Leuner, C., Dressman, J., Verreck, G., Peeters, J., Blaton, N., Augustijns, P., Kinget, R., Mooter, G.V.D., 2002. Thermal properties of hot-stage extrudates of itraconazole and Eudragit E100. J. Therm. Anal. Calorim. 68, 591–601.
Suzuki, N., Nakamura, Y., Watanabe, Y., Yasushi, K., 2001. Intercalation compounds of layered materials for drug delivery use. II. Diclofenac sodium. Chem. Pharm. Bull. 49, 964–968.
Tammaro, L., Costantino, U., Bolognese, A., Sammartino, G., Marenzi, G., Calignano, A., Tetè, S., Mastrangelo, F., Califano, L., Vittoria, V., 2007. Nanohybrids for controlled antibiotic release in topical applications. Int. J. Antimicrob. Agents 29, 417–423.
Uhl, F.M., Davuluri, S.P., Wong, S.-C., Webster, D.C., 2004. Organically modified montmirillonites in UV curable urethane acrylate films. Polymer 45, 6175–6187.
Vatier, J., Harman, A., Castela, N., Droy-Lefaix, M.T., Farinotti, R., 1994. Interactions of cimetidine and ranitidine with aluminum-containing antacids and a clay-containing gastric-protective drug in an artificial stomach–duodenum model. J. Pharm. Sci. 83, 962–966.
White, J.L., Hem, S.L., 1983. Pharmaceutical aspects of clay–organic interactions. Ind. Eng. Chem. Prod. Rd. 22, 665–671.
Wurster, D.E., Taylor, P.W., 1965. Dissolution rates. J. Pharm. Sci. 54, 169–175.
Yang, M., Wang, P., Huang, C.-Y., Ku, M.S., Liu, H., Gogos, C., 2010. Solid dispersion of acetaminophen and poly(ethylene oxide) prepared by hot-melt mixing. Int. J. Pharm. 395, 53–63.